arXiv:0803.2723v1 [quant-ph] 18 Mar 2008

Metastability Driven by Soft Quantum Fluctuation Modes

Marco Zoli

Istituto Nazionale Fisica della Materia - Dipartimento di Fisica

Universitá di Camerino, 62032, Italy. - marco.zoli@unicam.it

(Dated: March 20, 2008)

Abstract

The semiclassical Euclidean path integral method is applied to compute the low temperature quantum decay rate for a particle placed in the metastable minimum of a cubic potential in a *finite* time theory. The classical path, which makes a saddle for the action, is derived in terms of Jacobian elliptic functions whose periodicity establishes the one-to-one correspondence between energy of the classical motion and temperature (inverse imaginary time) of the system. The quantum fluctuation contribution has been computed through the theory of the functional determinants for periodic boundary conditions. The decay rate shows a peculiar temperature dependence mainly due to the softening of the low lying quantum fluctuation eigenvalues. The latter are determined by solving the Lamè equation which governs the fluctuation spectrum around the time dependent classical bounce.

Keywords: Low Temperature Decay Rate, Path Integral Methods, Quantum Fluctuations, Soft Modes

PACS numbers: 03.65.Sq, 03.75.Lm, 05.30.-d, 31.15.xk

1. Introduction

Quantum tunneling from a metastable state through a potential barrier is a fundamental nonlinear phenomenon occuring in many branches of the physical sciences [1, 2, 3, 4, 5, 6, 7, 8, 9]. The standard semiclassical approach to metastability has been formulated since long by Langer [10] and Coleman [11] in the fields of statistical and nuclear physics respectively. The main idea underlying such approach consists in selecting a classical background which solves the Euler-Lagrange equation and makes a saddle point for the action. Around the background, the quantum fluctuations are treated in quadratic approximation and their spectrum is obtained by solving a Schrödinger like stability equation whose potential is given by the second spatial derivative of the metastable potential. The semiclassical method finds a concise and powerful description in the Euclidean path integral formalism [12, 13] in which the time for the bounce to perform a full excursion (inside the classically allowed region) is a measure of the inverse temperature of the system. In the standard treatments of metastability [10, 11], it is assumed that such time is *infinite* and therefore the decay rate formula holds, strictly speaking, only at $T = 0$. For applications to specific systems however, a precise knowledge of the decay rate at finite T (but within the quantum tunneling regime) may be of great interest. To this purpose one has to build the *finite* time theory of metastability for specific nonlinear potentials, setting the crossover temperature between (low T) quantum and (high T) activated regimes and find the shape of the decay rate when the crossover is approached from below. Focussing on a widely investigated model in nonlinear science, a particle in the one dimensional cubic potential, I present in Section 2 the finite time solution of the Euler-Lagrange equation in terms of the powerful Jacobian elliptic functions formalism [14]: this generalizes the well known *infinite* time bounce which is recovered asymptotically. I emphasize that the system is taken as non dissipative therefore the *temperature* should not be viewed here as a property of the heat bath [15, 16, 17], but rather as a measure of the system size along the time axis. Section 3 is devoted to the computation of the classical action. Section 4 describes the method of the semiclassical path integral and presents the calculation of the overall quantum fluctuation contribution through the theory of the functional determinants. Section 5 solves the stability equation for the periodic potential defined by the classical background. This permits to obtain analytically the lowest quantum fluctuation eigenvalues as a function of the finite time/temperature. It

is shown in Section 6 that the softening of such eigenvalues close to the crossover largely determines the peculiar shape of the decay rate and its deviation from the prediction of the standard zero T theory. The conclusions are drawn in Section 7.

2. Cubic Potential Model

To begin, consider a particle of mass M in the one dimensional cubic anharmonic potential:

$$V(x) = \frac{M\omega^2}{2}x^2 - \frac{\gamma}{3}x^3 \ , \tag{1}$$

plotted in Fig. 1(a) for $\hbar\omega = 20meV$ and $M = 10^3 m_e$, m_e being the electron mass. Say a the position of the top of barrier whose height is $V(a) = \gamma a^3/6$ with $\gamma = M\omega^2/a$. Let's take throughout the paper, $a = 1\mathring{A}$. At $x = 0$ the particle is in a local minimum from which it cannot escape classically. Thus, in the real time formalism, the classical equation of motion admits only the trivial solution $x_{cl} = 0$. Physically however such local minimum is metastable as quantum fluctuations allow the particle to explore the abyss at $x \geq 3a/2$. In fact, a non trivial classical solution can be found in the Euclidean space. Performing a Wick rotation from the real to the imaginary time, $t \to -i\tau$, the equation of motion reads:

$$M\ddot{x}_{cl}(\tau) = V'(x_{cl}(\tau)) \ , \tag{2}$$

where V' means derivative with respect to x_{cl}. In the spirit of the semiclassical method, the particle path $x(\tau)$ has been split in the sum of a classical and a quantum component, $x(\tau) = x_{cl}(\tau) + \eta(\tau)$. The Wick rotation is equivalent to turn the potential upside down with respect to the real time as shown in Fig. 1(b). Now it is clear that the classical motion can take place in the reversed potential: precisely, the particle moves back and forth between the turning points x_1 and x_2 in which the particle velocity vanishes.

Integrating Eq. (2), one gets:

$$\frac{M}{2}\dot{x}_{cl}^2(\tau) - V(x_{cl}(\tau)) = E \ , \tag{3}$$

with the constant E representing the classical energy. Defining:

$$\begin{aligned}
\chi_{cl}(\tau) &= \frac{2}{3}\frac{x_{cl}(\tau)}{a} \\
\kappa &= \frac{4E}{27V(a)} \ ,
\end{aligned} \tag{4}$$

Eq. (3) is easily integrated to yield:

$$\tau - \tau_0 = \pm\frac{1}{\omega}\int_{\chi_{cl}(\tau_0)}^{\chi_{cl}(\tau)} \frac{d\chi}{\sqrt{-\chi^3 + \chi^2 + \kappa}} \ , \tag{5}$$

where τ_0 is the center of motion between the turning points. The boundary conditions on the classical motion define a physical picture in which the particle starts from x_2 at the time $\tau = -L/2$, reaches x_1 at $\tau = \tau_0$ and returns to the initial position at $\tau = L/2$. Then, Eq. (5) has a time reversal invariant solution whose period L is finite and dependent on E.

Looking at Fig. 1(b), one sees that the amplitude $x_1 - x_2$ attains the largest value for the $E = 0$ motion while x_2 and x_3 coincide. For $E < 0$ motions, x_3 is negative. The turning points x_1, x_2, x_3 are given by the zeros of the equation $-\chi^3 + \chi^2 + \kappa = 0$ ($\chi \equiv 2x/(3a)$) which admits three real solutions for $\kappa \in [-4/27, 0]$, that is for $E \in [-V(a), 0]$. After some algebra I find:

$$\begin{aligned}
\chi_1 &= \frac{1}{3} + \frac{2}{3}\cos(\vartheta) \\
\chi_2 &= \frac{1}{3} + \frac{2}{3}\cos(\vartheta - 2\pi/3) \\
\chi_3 &= \frac{1}{3} + \frac{2}{3}\cos(\vartheta - 4\pi/3) \\
\vartheta &= \frac{1}{3}\arccos\Bigl(\frac{27\kappa}{2} + 1\Bigr) \ .
\end{aligned} \tag{6}$$

At the bounds of the energy range, Eq. (6) yields:

$$\begin{aligned}
&\mathbf{E} = \mathbf{0} \Rightarrow \chi_1 = 1; \ \chi_2 = \chi_3 = 0 \\
&\mathbf{E} = -\mathbf{V}(\mathbf{a}) \Rightarrow \chi_1 = \chi_2 = 2/3; \ \chi_3 = -1/3 \ .
\end{aligned} \tag{7}$$

Thus, at the sphaleron energy $E_{sph} = |E| = V(a)$, the amplitude of the finite time solution has to shrink into a point. Let's find the general solution of Eq. (5) by pinning the center of motion at $\chi_{cl}(\tau_0) = \chi_1$ and using the result [18]:

$$\begin{aligned}
&\int_{\chi_{cl}(\tau)}^{\chi_1} \frac{d\chi}{\sqrt{(\chi_1 - \chi)(\chi - \chi_2)(\chi - \chi_3)}} = \frac{2F(\lambda, p)}{\sqrt{\chi_1 - \chi_3}} \\
&\lambda = \arcsin\left(\sqrt{\frac{\chi_1 - \chi_{cl}(\tau)}{\chi_1 - \chi_2}}\right) \\
&p = \sqrt{\frac{\chi_1 - \chi_2}{\chi_1 - \chi_3}} \ ,
\end{aligned} \tag{8}$$

where $F(\lambda, p)$ is the elliptic integral of the first kind with amplitude λ and modulus p. Then, through Eqs. (4), (5), (8), I derive the bounce solution of the *finite time* theory:

$$\begin{aligned}
&x_{cl}(\tau) = \frac{3a}{2}\big[\chi_1 cn^2(\varpi, p) + \chi_2 sn^2(\varpi, p)\big] \\
&\varpi = \sqrt{\chi_1 - \chi_3}\,\frac{\omega}{2}(\tau - \tau_0) \ ,
\end{aligned} \tag{9}$$

$sn(\varpi, p)$ and $cn(\varpi, p)$ are the *sine*- and *cosine*- amplitudes respectively [14]. The modulus p keeps tracks of the classical mechanics through the second of Eq. (4) and Eq. (6).

At $\mathbf{E = 0,\ p = 1}$, the bounce of the *infinite time* theory is recovered:

$$x_{cl}(\tau) = \frac{3a}{2} cn^2(\varpi, 1) = \frac{3a}{2} sech^2\big(\frac{\omega}{2}(\tau - \tau_0)\big) \ . \tag{10}$$

At $\mathbf{E_{sph}, p = 0}$, the bounce solution is (as expected) a point-like object set at the bottom of the valley in the reversed potential: $x_{cl}(\tau) = a$. Thus, Eq. (9) defines the transition state which is a saddle for the action below the sphaleron. Computation of Eq. (9), shows that the bounce amplitude contracts by increasing the *energy over potential height* ratio (in absolute value). As the bounce is a combination of squared Jacobi elliptic functions, its period is $2K(p)$ with $K(p) = F(\pi/2, p)$ being the complete elliptic integral of the first kind [14]. Hence, from Eq. (9), I get:

$$\sqrt{\chi_1 - \chi_3}\,\frac{\omega}{4} L = K(p) \ , \tag{11}$$

which establishes the relation between the oscillation period and the classical energy embedded in the turning points. As stated in the Introduction, one can map the imaginary time onto the temperature axis, $L = \hbar/(K_B T^*)$, where T^* is the temperature at which the particle makes the excursion to and from the edge of the abyss for a given E. Then, only periodic bounces whose period is proportional to the inverse temperature determine the decay rate and the *finite time* theory can be viewed as a finite T^* theory. From Eq. (11) I get:

$$K_B T^* = \frac{\hbar\omega}{4} \frac{\sqrt{\chi_1 - \chi_3}}{K(p)} \ . \tag{12}$$

Eq. (12) is plotted in Fig. 2 on a linear scale. Approaching $E = 0$, T^* consistently drops to zero while the value at E_{sph} defines the transition temperature T_c^* between quantum and activated regimes.

Analytically, at the sphaleron, Eq. (12) yields

$$K_B T_c^* = \frac{\hbar\omega}{2\pi} \ , \tag{13}$$

which represents the upper bound for the occurence of quantum tunneling and precisely sets the Goldanskii criterion [19, 20] for a cubic anharmonic potential. Taking $\hbar\omega = 20meV$, I get $T_c^* = 36.938K$. The following calculations are carried out in the low temperature range up to T_c^*.

3. Classical Action

The classical action $A[x_{cl}]$ for the bounce in the finite time theory can be computed in terms of the path velocity $\dot{x}_{cl}(\tau)$ by the relations:

$$
\begin{aligned}
A[x_{cl}] =&\ MN^{-2} - E \cdot L(E) \\
N^{-2} =&\ 2\int_0^{L/2} d\tau[\dot{x}_{cl}(\tau)]^2 \\
\dot{x}_{cl}(\tau) =&\ \frac{3a}{2}\mathcal{F} \cdot sn(\varpi, p)cn(\varpi, p)dn(\varpi, p) \\
\mathcal{F} =&\ -\omega(\chi_1 - \chi_2)\sqrt{\chi_1 - \chi_3}\ ,
\end{aligned}
\tag{14}
$$

where $dn(\varpi, p)$ is the *delta*- amplitude [14].

Computation of Eq. (14) requires knowledge of $L(E)$ through Eqs. (4), (6) and (11).

In the $E \to 0$ limit, from Eq. (14), I get the result

$$
\frac{A[x_{cl}]}{\hbar} \to \frac{6M^3\omega^5}{5\hbar\gamma^2}\ ,
\tag{15}
$$

which serves as testbench for the computational method. The dependence of the classical action on $1/\gamma^2$ reflects the well known fact that metastable systems are non perturbative and provides the fundamental motivation for the semiclassical treatment. Eq. (15) permits to set the potential parameters such as the condition $A[x_{cl}] > \hbar$ holds and the semiclassical method is thus justified. As M and a have been taken constant, $A[x_{cl}] \propto \omega$ in the $E \to 0$ limit.

The classical action and the squared norm of the path velocity (times M) are displayed in Fig. 3(a) and Fig. 3(b) respectively. While, at low T^*, the two plots are essentially identical the role of the term $E \cdot L(E)$ in Eq. (14) becomes more significant at increasing T^*. At T^*_c, N^{-2} vanishes whereas $A[x_{cl}]$ is finite. Note that $A[x_{cl}]$ decreases smoothly versus T^* confirming that the transition to the activated regime at T^*_c is of second order as suggested long ago [20, 21].

In general, the criterion to establish the order of the transitions in periodic tunneling systems has been formulated by Chudnovsky [22] through the behavior of the oscillation period $L(E)$: *i)* a monotonic $L(E)$ below the sphaleron implies $A[x_{cl}] < A_0$ for $T^* < T^*_c$, with A_0 being the thermal action given by $A_0 = \hbar V(a)/K_B T^*$. At $T^* = T^*_c$, both conditions $A[x_{cl}] = A_0$ and $dA[x_{cl}]/dT = dA_0/dT$ are fulfilled hence the crossover from the quantum to the thermal regime is expected to be smooth; *ii)* on the other hand, a nonmonotonic behavior of $L(E)$ would indicate a sharp transition. As it can deduced from Fig. 2, $L(E)$

increases versus $E \in [-V(a), 0]$, thus the case *i)* applies to the cubic potential in Eq. (1) and, consistently, the action is convex upwards versus T^*. At the sphaleron, I find numerically: $L(E_{sph})/\hbar = 0.314 meV^{-1}$. Note, from Eq. (11), that such value corresponds to $2\pi/\hbar\omega$ (being $K(p=0) = \pi/2$) and this proves the correctness of the computation. In fact at E_{sph} the bounce is a point, that is a static solution of Eq. (3) but, near E_{sph}, the periodic path is the sum of the sphaleron and a fluctuation with negative eigenvalue ε_{-1} whose period tends to $L(E_{sph}) = 2\pi/\sqrt{|\varepsilon_{-1}|}$ [23, 24]. Then one infers that, for $|E| \to E_{sph}$, the ground state eigenvalue has to behave as: $\varepsilon_{-1} \to -\omega^2$. This key point will be further investigated in Section 5.

4. Semiclassical Euclidean Path Integral

This Section presents the calculation of the space-time Euclidean path integral between the positions x_i and x_f connected in the time L. In the semiclassical model and treating the quantum fluctuations in quadratic approximation, the path integral reads:

$$
\begin{aligned}
< x_f|x_i >_L &= \exp\left[-\frac{A[x_{cl}]}{\hbar}\right] \cdot \int D\eta \exp\left[-\frac{A_f[\eta]}{\hbar}\right] \\
A_f[\eta] &= \int_{-L/2}^{L/2} d\tau \left(\frac{M}{2}\dot{\eta}^2(\tau) + \frac{1}{2}V''(x_{cl}(\tau))\eta^2(\tau)\right) \\
V''(x_{cl}(\tau)) &= M\omega^2\left(1 - \frac{2}{a}x_{cl}(\tau)\right) .
\end{aligned}
\tag{16}
$$

Thus, to get the quantum fluctuation action $A_f[\eta]$, one has to solve a second order differential problem which, after partial integration in the first term, is formulated as follows:

$$
\begin{aligned}
\hat{O}\eta_n(\tau) &= \varepsilon_n \eta_n(\tau) \\
\hat{O} &\equiv -\partial_\tau^2 + V''(x_{cl}(\tau))/M \\
\eta(\tau) &= \sum_{n=-1}^{\infty} \varsigma_n \eta_n(\tau) ,
\end{aligned}
\tag{17}
$$

where the ε_n are the quantum fluctuation eigenvalues while the coefficients ς_n of the series expansion in ortonormal components $\eta_n(\tau)$ define the measure of the fluctuation paths integration in Eq. (16):

$$\int D\eta = \aleph \prod_{n=-1}^{\infty} \int_{-\infty}^{\infty} \frac{d\varsigma_n}{\sqrt{2\pi\hbar/M}} \ , \tag{18}$$

$\aleph$ depends only on the functional integral measure.

First, observe from Eq. (2) that $\dot{x}_{cl}(\tau)$ satisfies the homogeneous equation associated to the second order Schrödinger-like differential operator $\hat{O}\eta_n(\tau) = 0$. This is a general consequence of the τ-translational invariance of the system. Hence, $\dot{x}_{cl}(\tau)$ is proportional to the ortonormal eigenmode $\eta_0(\tau)$, ($\eta_0(\tau) \equiv N\dot{x}_{cl}(\tau)$) with $\varepsilon_0 = 0$. The latter however cannot be the ground state as the bounce solution (Eq. (9)) is non monotonic and $\dot{x}_{cl}(\tau)$ has one node along the time axis within the period L. This implies that the quantum fluctuation spectrum has one negative eigenvalue corresponding to the ground state [25]. Here lies the origin of metastability. Second, from Eq. (14), note that for any two points ϖ_1, ϖ_2 such that $\varpi_2 = \varpi_1 \pm 2K(p)$, $\dot{x}_{cl}(\varpi_2) = \dot{x}_{cl}(\varpi_1)$. The important consequence is that the fluctuation eigenmodes obey periodic boundary conditions (PBC).

As x_i and x_f defined in Eq. (16) coincide for the periodic bounce, Eq. (16) represents the single bounce contribution Z_1 to the total partition function Z_T. In fact, the latter also contains the effects of all multiple (non interacting) excursions to and from the abyss which is equivalent to sum over an infinite number of single bounce contributions like Z_1. Moreover, also the static solution of Eq. (2), $x_{cl} = 0$ contributes to Z_T by the harmonic partition function Z_h which can be easily determined using the same measure in Eq. (18). Summing up, Z_T is given by

$$\begin{aligned} Z_T &= Z_h \exp(Z_1/Z_h) \\ Z_h &= \aleph |Det[\hat{h}]|^{-1/2} \ , \end{aligned} \tag{19}$$

$Det[\hat{h}]$ ($\hat{h} \equiv -\partial_\tau^2 + \omega^2$) is the harmonic fluctuation determinant. Being the decay rate Γ proportional to the imaginary exponential argument through the Feynman-Kac formula [2], it follows that there is no need to determine $\aleph$ as it cancels out in the ratio Z_1/Z_h.

Supposed to have solved Eq. (17), the quantum fluctuation term in Eq. (16) can be worked out by carrying out Gaussian path integrals. Formally one gets:

$$
\begin{aligned}
&\int D\eta \exp\left[-\frac{A_f[\eta]}{\hbar}\right] = \aleph \cdot Det\left[\hat{O}\right]^{-1/2} \\
&Det[\hat{O}] \equiv \prod_{n=-1}^{\infty} \varepsilon_n \ .
\end{aligned}
\tag{20}
$$

The evaluation of Eq. (20) is carried out through the two following steps.

A. Zero Mode

The Gaussian approximation leading to Eq. (20) is broken by the Goldstone mode arising from the fact that τ_0, the center of the bounce, can be located arbitrarily inside L. The technique to overcome the obstacle is well known [20]: the divergent integral over the coordinate $d\varsigma_0$ associated to the zero mode in the measure $D\eta$ is transformed into a $d\tau_0$ integral. Accordingly the eigenvalue $\varepsilon_0 = 0$ is extracted from $Det[\hat{O}]$ and its contribution to Eq. (20) is replaced as follows

$$
(\varepsilon_0)^{-1/2} \rightarrow \sqrt{\frac{MN^{-2}}{2\pi\hbar}} L \ .
\tag{21}
$$

To be rigorous, this replacement holds in the approximation of quadratic fluctuations [26] while higher order terms may be significant around the crossover. It is also worth noticing that Eq. (21) is often encountered in the form $(\varepsilon_0)^{-1/2} \rightarrow \sqrt{\frac{A[x_{cl}]}{2\pi\hbar}} L$. However the latter is correct only in the low T limit where $A[x_{cl}]$ equals MN^{-2} (as made clear by Fig. 3) while, approaching T_c^*, the difference between the two objects gets large. This fact is crucial in establishing the behavior of the decay rate at the crossover as shown in Section 6.

Thus, handled the zero mode, I turn to the evaluation of the regularized determinant $Det^R[\hat{O}]$ defined by $Det[\hat{O}] = \varepsilon_0 \cdot Det^R[\hat{O}]$.

B. Regularized Fluctuation Determinant

The calculation of $Det^R[\hat{O}]$ is based on the theory of functional determinants for second order differential operators which was first developed for Dirichlet boundary conditions [27] and then extended to general operators and boundary conditions in several ways [28, 29, 30].

As a fundamental feature, to evaluate $Det^R[\hat{O}]$ one has to know only the classical path which makes the action stationary. As shown above the path velocity obeys PBC for any two points ϖ_1, ϖ_2 separated by the period $2K(p)$. The latter corresponds to the oscillation period L along the τ-axis. It can be easily checked that also the path acceleration fulfills the PBC. Then, the regularized determinant is given by [29]:

$$Det^R[\hat{O}] = \frac{< f_0|f_0 > \big(f_1(\varpi_2) - f_1(\varpi_1)\big)}{f_0(\varpi_1)W(f_0, f_1)} \ , \tag{22}$$

where f_0, f_1 are two independent solutions of the homogeneous equation: $\hat{O}\eta_n(\tau) = 0$. f_0 is obviously $\dot{x}_{cl}$ while f_1 can be taken as:

$$f_1 = \frac{\partial x_{cl}}{\partial q} \ ; \ q \equiv p^2 \ , \tag{23}$$

$W(f_0, f_1)$ is their Wronskian and $< f_0|f_0 > \equiv N^{-2}$ is given by Eq. (14).

The Wronskian, being constant along τ, can be calculated in any convenient point. Let's take τ_0 as $f_0(\tau_0) = 0$. Then:

$$\begin{aligned} W(f_0, f_1)\Big|_{\tau_0} &= -\dot{f}_0(\tau_0) f_1(\tau_0) \\ &= \frac{9}{8} a^2 \omega^2 (\chi_1 - \chi_2)(\chi_1 - \chi_3) \frac{\partial \chi_1}{\partial q} \ . \end{aligned} \tag{24}$$

Working out the calculation, $Det^R[\hat{O}]$ in Eq. (22) transforms into:

$$\begin{aligned} Det^R[\hat{O}] &= \frac{2}{\omega\sqrt{\chi_1 - \chi_3}\bar{p}^2} \left[\frac{E(\pi/2, p) - \bar{p}^2 K(p)}{p^2} \right] \cdot \frac{< f_0|f_0 >}{W(f_0, f_1)} \\ \bar{p}^2 &= 1 - p^2 \ , \end{aligned} \tag{25}$$

which can be directly computed using Eqs. (14), (24). $E(\pi/2, p)$ is the complete elliptic integral of the second kind [14].

It is however known in the theory of functional determinants [26, 27] that only ratios of determinants are meaningful in value and sign, such ratios arising naturally in the path integral method as it has been pointed out above. In fact, $Det^R[\hat{O}]$ would diverge in the

$T^* \to 0$ limit due to the fact that the determinant is the product over an infinite number of eigenvalues with magnitude greater than one. Consistently with Eq. (19), $Det^R[\hat{O}]$ has to be normalized over $Det[\hat{h}]$ which, in the case of PBC, is: $Det[\hat{h}] = -4\sinh^2(\omega L/2)$ [29]. The normalization cancels the exponential divergence and makes the ratio finite.

Then, observing that for $E \to 0$ ($T^* \to 0$):

$$
\begin{aligned}
& W(f_0, f_1)\Big|_{\tau_0} \to \frac{9}{8}a^2\omega^2(1-p^2) \\
& < f_0|f_0 > \to \frac{6}{5}a^2\omega \\
& K(p) \to \ln(4/\sqrt{1-p^2}) \ ,
\end{aligned}
\tag{26}
$$

from Eq. (25), I finally get the finite ratio

$$
\frac{Det^R[\hat{O}]}{Det[\hat{h}]} \to -\frac{1}{60\omega^2} \ . \tag{27}
$$

The dimensionality $[\omega^{-2}]$ correctly accounts for the fact that one eigenvalue has been extracted from $Det^R[\hat{O}]$. From the computation of Eq. (25), the following informations can be extracted:

1) the $T^* \to 0$ limit given by Eq. (27) is in fact an excellent estimate up to $T^* \sim T_c^*/2$ whereas a strong deviation is found at larger T^* up to $\sim T_c^*$.

2) The ratio $Det^R[\hat{O}]/Det[\hat{h}]$ is negative for any T^* and this sign has physical meaning as it is due precisely to the negative ground state eigenvalue ε_{-1} of the fluctuation spectrum. As Z_1/Z_h contributes to the partition function by the square root of the fluctuation (inverse) determinants ratio it follows that such contribution is purely imaginary.

Moreover, close to the sphaleron, $T^* \sim T_c^*$, $< f_0|f_0 > \propto p^4$ and $W(f_0, f_1) \propto p^2$, thus $Det^R[\hat{O}]$ tends to zero as $Det^R[\hat{O}] \propto p^2$. The fact that $Det^R[\hat{O}]$ vanishes at the crossover causes the divergence of the inverse ratio. This divergence may look surprising since the zero mode had been extracted from the determinant: physically one realizes that there must be a quantum fluctuation mode (ε_1) which softens by increasing T^* and ultimately vanishes at the sphaleron.

To understand in detail the key effects of the low lying fluctuation eigenvalues ε_1 and ε_{-1}, one has to determine them analytically by solving the stability equation in Eq. (17). This is done in the next Section.

5. Lamè Equation

Take Eq. (17) with the second derivative of the potential given in Eq. (16). Using Eq. (9) and working out the algebra, I get the stability equation which governs the fluctuation spectrum around the classical background:

$$
\begin{aligned}
&\frac{d^2}{d\varpi^2}\eta_n(\tau) = \big[l(l+1)p^2 sn^2(\varpi, p) + \mathcal{A}_n\big]\eta_n(\tau) \\
&\mathcal{A}_n = \frac{4(1-3\chi_1)}{\chi_1 - \chi_3} - \frac{4\varepsilon_n}{\omega^2(\chi_1 - \chi_3)} \\
&l(l+1) \equiv 12 \; .
\end{aligned}
\tag{28}
$$

This is the Lamè equation in the Jacobian form for the case $l = 3$ [31]. For a given l and p, Eq. (28) yields periodic solutions (which can be expanded in infinite series) for an infinite sequence of characteristic $\mathcal{A}_n$ values. The continuum of the fluctuation spectrum stems from this sequence. However, being l positive and integer, the first $2l + 1$ solutions of Eq. (28) are not infinite series but polynomials in the Jacobi elliptic functions with real period $2K(p)$ or $4K(p)$. Being the period of the potential, $2K(p)$ plays the role of a lattice constant.

Then, Eq. (28) admits seven polynomial solutions with eigenvalues $\mathcal{A}_n, n \in [-l, l]$, from which the corresponding ε_n are derived. However not all the ε_n are good fluctuation eigenvalues. In fact four out of seven have to be discarded as their eigenfunctions do not fulfill the PBC required for the fluctuation components: $\eta_n(\varpi_1) = \eta_n(\varpi_1 \mp 2K(p))$. Thus, the three good eigenmodes and relative eigenvalues in polynomial form are:

$$
\begin{aligned}
&\eta_0 \propto \; sn(\varpi, p)cn(\varpi, p)dn(\varpi, p) \\
&\varepsilon_0 = \; 0 \\
&\eta_1 \propto \; (sn^2\varpi - p^{-2})^{1/2}\left[sn^2\varpi + \frac{2}{p^2 + \mathcal{A}_1}\right] \\
&\varepsilon_1 = \; \omega^2\Big(\alpha_1 - \alpha_2\mathcal{A}_1\Big) \\
&\eta_{-1} \propto \; (sn^2\varpi - p^{-2})^{1/2}\left[sn^2\varpi + \frac{2}{p^2 + \mathcal{A}_{-1}}\right] \\
&\varepsilon_{-1} = \; \omega^2\Big(\alpha_1 - \alpha_2\mathcal{A}_{-1}\Big) \\
&\mathcal{A}_1 = -(2 + 5p^2) - 2\sqrt{4p^4 - p^2 + 1} \\
&\mathcal{A}_{-1} = -(2 + 5p^2) + 2\sqrt{4p^4 - p^2 + 1} \\
&\alpha_1 \equiv \; 1 - 3\chi_1 \\
&\alpha_2 \equiv \; \frac{\chi_1 - \chi_3}{4} \; .
\end{aligned}
\tag{29}
$$

The plots of ε_1 and ε_{-1} versus the *energy over potential height* ratio are reported on Fig. 4(a) and Fig. 4(b) respectively. Note that:

i) $\varepsilon_0 = 0$ is the zero mode eigenvalue correctly recovered through the stability equation.

ii) ε_1 lies in the continuum and, as it can be easily deduced from Eq. (29), it drops to zero close to the sphaleron as $\varepsilon_1 \propto p^2$: this is precisely the behavior previously envisaged for $Det^R[\hat{O}]$. Hence, ε_1 is the soft mode driving the enhancement in the decay rate below the sphaleron which is discussed in the next Section. Observe that, for $p \to 0$, $K(p) \simeq \pi/2 + \pi p^2/8$. Then, by Eq. (12), close to the crossover: $\varepsilon_1 \propto T_c^* - T^*$. At T_c^*, ε_1 and ε_0 merge consistently with the double degeneracy of the corresponding eigenmodes above the crossover.

iii) ε_{-1} is the negative eigenvalue responsible for metastability. ε_{-1} also softens (in absolute value) with respect to the value $\varepsilon_{-1} = -5\omega^2/4$ found at $E = 0$. Interestingly, along the temperature scale, the substantial reduction starts up at $T^* \sim T_c^*/2$, that is in the same range at which the classical properties deviate from the predictions of the infinite time theory. Finally, at the sphaleron, from Eq. (29) I get $\varepsilon_{-1} = -\omega^2$ thus confirming the prediction made at the end of Section 3. This completes the analysis of the soft eigenvalues which ultimately govern the quantum fluctuation spectrum.

6. Decay Rate

The decay rate Γ of a metastable state is given in semiclassical theory by

$$\Gamma = A \exp(-B/\hbar)[1 + O(\hbar)] \ , \tag{30}$$

where A and B depend on the specific shape of the potential. The investigation carried out so far allows us to identify the coefficients A and B in Eq. (30) with $\hbar\sqrt{|Det[\hat{h}]/Det[\hat{O}]|}/L$ and $A[x_{cl}]$ respectively. Then, the general expression for the finite time/temperature $\Gamma(T^*)$ is:

$$\Gamma(T^*) = \hbar\sqrt{\frac{MN^{-2}}{2\pi\hbar}}\sqrt{\left|\frac{Det[\hat{h}]}{Det^R[\hat{O}]}\right|}\exp\left[-\frac{A[x_{cl}]}{\hbar}\right] \ . \tag{31}$$

Eq. (31) is plotted in Fig. 5 against temperature up to T^*_c for three oscillator energies. While at low T^*, $\Gamma(T^*)$ merges with the constant decay rate of the *infinite time* theory, an increase of $\Gamma(T^*)$ is found in all plots above $T^* \sim T^*_c/2$ where the combined effects of quantum fluctuations and classical action softening become evident. Approaching the crossover, $\Gamma(T^*)$ deviates from the $T = 0$ result and reaches a peak value $\Gamma(T^*_P)$ which is larger for lower ω. This effect is mainly ascribable to the soft eigenvalue ε_1. Note however that for $\hbar\omega = 10meV$, $\Gamma(T^*_P)/\hbar\omega \sim 1$, signalling that the application of the semiclassical method itself becomes questionable. In fact, as noted below Eq. (15), the latter works when $A[x_{cl}] > \hbar$ and such condition starts to be well fulfilled by the case $\hbar\omega = 20meV$ as shown in Fig. 3. Clearly the ω values making the semiclassical method feasible also depend on M which has been assumed light in the present discussion. Heavvier particle masses favor the condition $\Gamma(T^*_P)/\hbar\omega < 1$ and sustain the applicability of the semiclassical method over a broader range of ω.

Above T^*_P the decay rate smoothly merges with the classical Arrhenius factor as $A[x_{cl}]/\hbar \to V(a)/K_B T^*_c$. The temperatures T^*_A, corresponding to the symbols in Fig. 5, mark the effective values at which quantum and thermal decay rates overlap. Beyond T^*_A and approaching T^*_c, the decay rate falls to zero as $\Gamma(T^*) \propto (T^*_c - T^*)^{1/2}$ and the quantum tunneling ceases to exist. The latter power law dependence is driven by $\sqrt{N^{-2}/Det^R[\hat{O}]} \propto p$.

The increase found for the quantum decay rate up to T_P^* and the subsequent sharp drop is interesting also in view of a comparison with activated systems described by classical Ginzburg-Landau finite size models [32, 33] in which spatio-temporal noise induces transitions between locally stable states of a nonlinear potential [34]. The changes in radius and the stability conditions of metastable metallic nanowires are an example of current interest [35, 36]. In classical systems of finite size L a power-law divergence in the escape rate (with critical exponent $1/2$) is predicted once a critical lenghtscale L_c is approached at fixed T [37]. Instead, the quantum decay rate of Eq. (31) cannot be divergent as the small parameter is $\hbar$ which, unlike the noise in classical systems, cannot be varied as a function of L at fixed T (or vice-versa) [38]. Accordingly the quantum tunneling decay rate is small and continuous.

Finally, it is worth pointing out that the decay rate may be computed *independently* of the squared norm N^{-2} as the latter cancels out in Eq. (31) by explicitly inserting Eq. (22). For this reason the behavior of the decay rate essentially depends on $Det^R[\hat{O}]/N^{-2}$ consistently with the quadratic approximation for the quantum fluctuations which enters the calculation at two stages: *a)* it determines the form of the quantum action in Eq. (16) and accordingly leads to Eq. (20); *b)* it allows us to replace the inverse zero mode eigenvalue by the squared norm of the bounce velocity, via Eq. (21).

7. Conclusion

I have developed the finite time (temperature) semiclassical theory for the quantum decay rate of a particle in the metastable state of a cubic potential model. In the Euclidean path integral formalism, the optimal escape trajectory emerges as the solution of the Euler-Lagrange equation in terms of Jacobian elliptic functions. Such solution is a time dependent bounce whose periodicity naturally leads to relate the temperature T^* to the energy of the classical motion. Consistently one defines the crossover temperature T_c^* between quantum and activated regimes which depends only on the fundamental oscillator frequency ω. As the path integral has been solved treating the quantum fluctuations in quadratic approximation, the calculations are confined to the low ω range, that is to the low temperature regime. In the numerical analysis I have considered a light particle mass and established, for this case, the lowest bound of ω values which make the semiclassical method reliable. The stumbling block in the calculation of the quantum decay rate is the estimate of the quantum fluctuation

effect in the *finite* time theory. In particular, I have *i)* derived a compact expression for the overall fluctuation contribution to the path integral in terms of the complete elliptic integrals and *ii)* solved the periodic stability equation which yields the low lying fluctuation eigenmodes and eigenvalues in polynomial form. The latter point permits to quantify the softening of the lowest positive and of the ground state (in absolute value) eigenvalues as T_c^* is approached. The softening of the lowest positive eigenvalue is mainly responsible for the enhancement in the quantum decay rate above the prediction of the infinite time (zero temperature) theory. The behavior of the decay rate has been studied in detail below T_c^*. At $T^* \sim T_c^*$, the thermal activation sets in while the quantum decay rate drops to zero according to the power law $\Gamma(T^*) \propto (T_c^* - T^*)^{1/2}$. Similar conclusions may be drawn by the analyses of a quartic metastable potential although the decay rate of the latter is smaller than in a cubic potential having the same structural parameters.

---

[1] L.D. Landau and E.M. Lifshitz, *Quantum Mechanics* 3^{rd} ed. Butterworth-Heinemann, Oxford (1977).

[2] L.S. Schulman *Techniques and Applications of Path Integration*, Wiley&Sons, New York (1981).

[3] H.A. Kramers, Physica **7**, 284 (1940).

[4] V.I. Melnikov and S.V. Meshkov, J. Chem. Phys. **85**, 1018 (1986).

[5] P. Hänggi, P. Talkner and M. Borkovec, Rev. Mod. Phys. **62**, 251 (1990).

[6] A. Barone and G. Paternò, *Physics and Applications of the Josephson Effect* , Wiley&Sons, New York (1982).

[7] A.I. Larkin and A. Varlamov, *Theory of Fluctuations in Superconductors*, Oxford University Press (2005).

[8] S.N. Burmistrov, L.B. Dubovskii and Y. Okuda, J. Low Temp. Phys. **138**, 55 (2005).

[9] J.D. Bao, L. Bi and Y. Jia, J. Chem. Phys. **126**, 204104 (2007).

[10] J.S. Langer, Ann. Phys. **41**, 108 (1967).

[11] S. Coleman, Phys. Rev. D **15**, 2929 (1977); C.G. Callan and S. Coleman, Phys. Rev. D **16**, 1762 (1977).

[12] R.P. Feynman, Rev. Mod. Phys. **20**, 367 (1948).

[13] R.P. Feynman and A.R. Hibbs, *Quantum Mechanics and Path Integrals*, Mc Graw-Hill, New York (1965).

[14] Z.X. Wang and D.R. Guo, *Special Functions*, World Scientific, Singapore (1989).

[15] H. Grabert and U. Weiss, Phys. Rev. Lett. **53**, 1787 (1984).

[16] P.S. Riseborough, P. Hänggi and E. Freidkin, Phys. Rev. A **32**, 489 (1985).

[17] N. Antunes, F.C. Lombardo, D. Monteoliva and P.I. Villar, Phys. Rev. E **73**, 066105 (2006).

[18] I.S. Gradshteyn and I.M. Ryzhik, *Tables of Integrals, Series and Products*, Academic Press, New York (1965).

[19] V.I. Goldanskii, Sov.Phys.Dokl. **4**, 74 (1959).

[20] A.I. Larkin and Y.N. Ovchinnikov, Sov.Phys.JETP **37**, 382 (1983); ibid. **59**, 420 (1984).

[21] I. Affleck, Phys. Rev. Lett. **46**, 388 (1981).

[22] E.M. Chudnovsky, Phys. Rev. A **46**, 8011 (1992).

[23] S.Y. Lee, H. Kim, D.K. Park and J.K. Kim, Phys. Rev. B **60**, 10086 (1999).

[24] D.A. Gorokhov and G. Blatter, Phys. Rev. B **56**, 3130 (1997).

[25] In bistable ϕ^4 potentials the classical path is monotonic and the zero mode is the ground state of the fluctuation spectrum.

[26] H. Kleinert, *Path Integrals in Quantum Mechanics, Statistics, Polymer Physycs and Financial Markets*, World Scientific Publishing, Singapore (2004).

[27] I.M. Gelfand and A.M. Yaglom, J.Math.Phys. **1**, 48 (1960).

[28] R. Forman, Invent.Math. **88**, 447 (1987).

[29] A.J. McKane and M.B. Tarlie, J.Math.Phys. **28**, 6931 (1995).

[30] K. Kirsten and A.J. McKane, J.Phys A:Math. Gen. **37**, 4649 (2004).

[31] E.T. Whittaker and G.N. Watson, *A Course of Modern Analysis*, 4^{th} ed. Cambridge University Press, (1927).

[32] W.G. Faris and G. Jona-Lasinio, J. Phys. A **15**, 3025 (1982).

[33] Y. Tu, Phys. Rev. E **56**, R3765 (1997).

[34] J.R. Chaudhuri, D. Barik and S.K. Banik, Phys. Rev. E **74**, 061119 (2006).

[35] A.I. Yanson, I.K. Yanson and J.M. van Ruitenbeck, Nature **400**, 144 (1999).

[36] C.-H. Zhang, F. Kassubek and C.A. Stafford, Phys. Rev. B **68**, 165414 (2003).

[37] J. Bürki, C.A. Stafford and D.L. Stein, Phys. Rev. Lett. **95**, 090601 (2005).

[38] D.L. Stein, Brazilian J. Phys. **35**, 242 (2005).

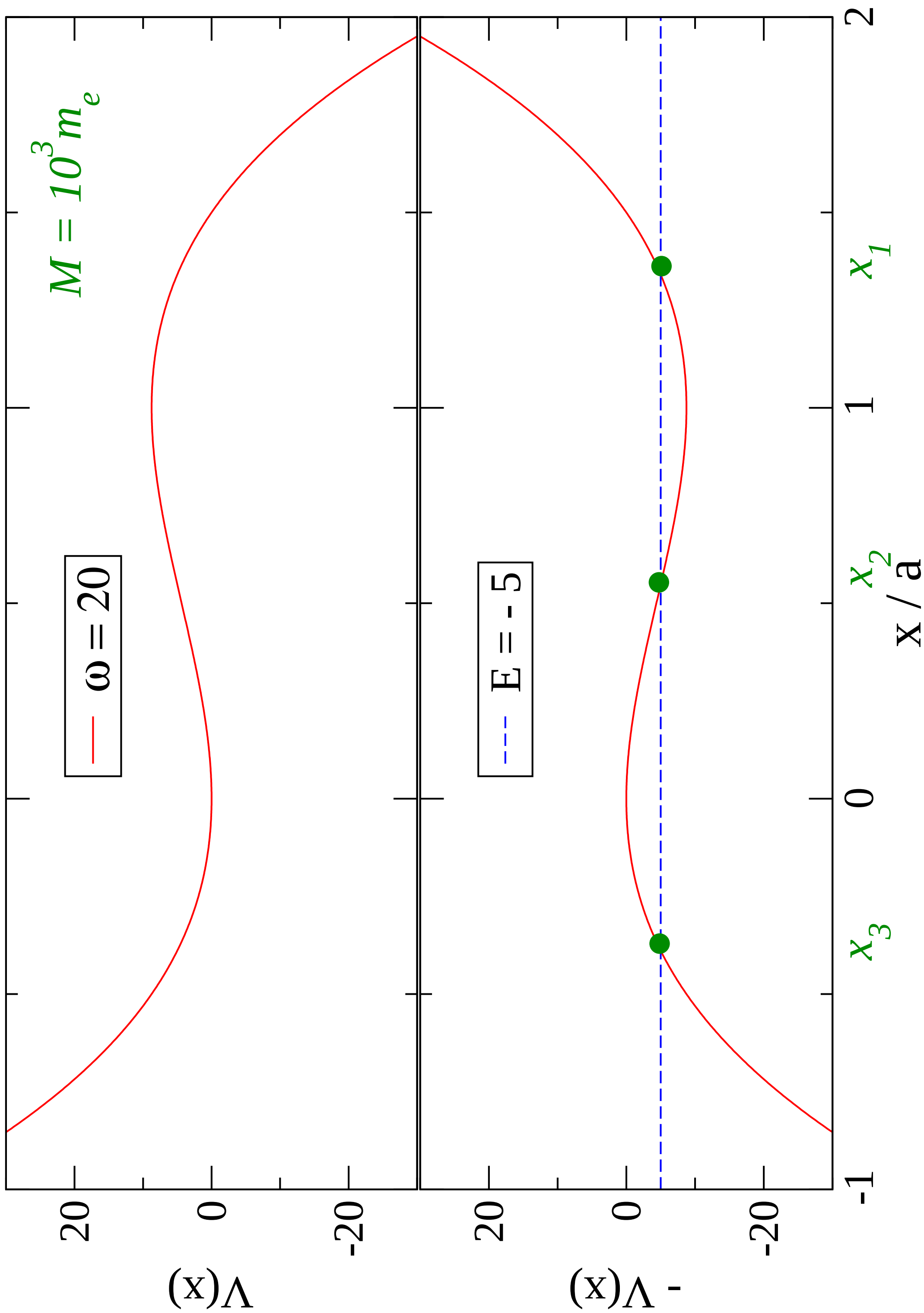

FIG. 1: (Color online) (a) Cubic potential in the real time representation, (b) Cubic potential in the imaginary time representation. ω is in meV. The intersections with the constant energy E (in meV) define the turning points for the classical motion.

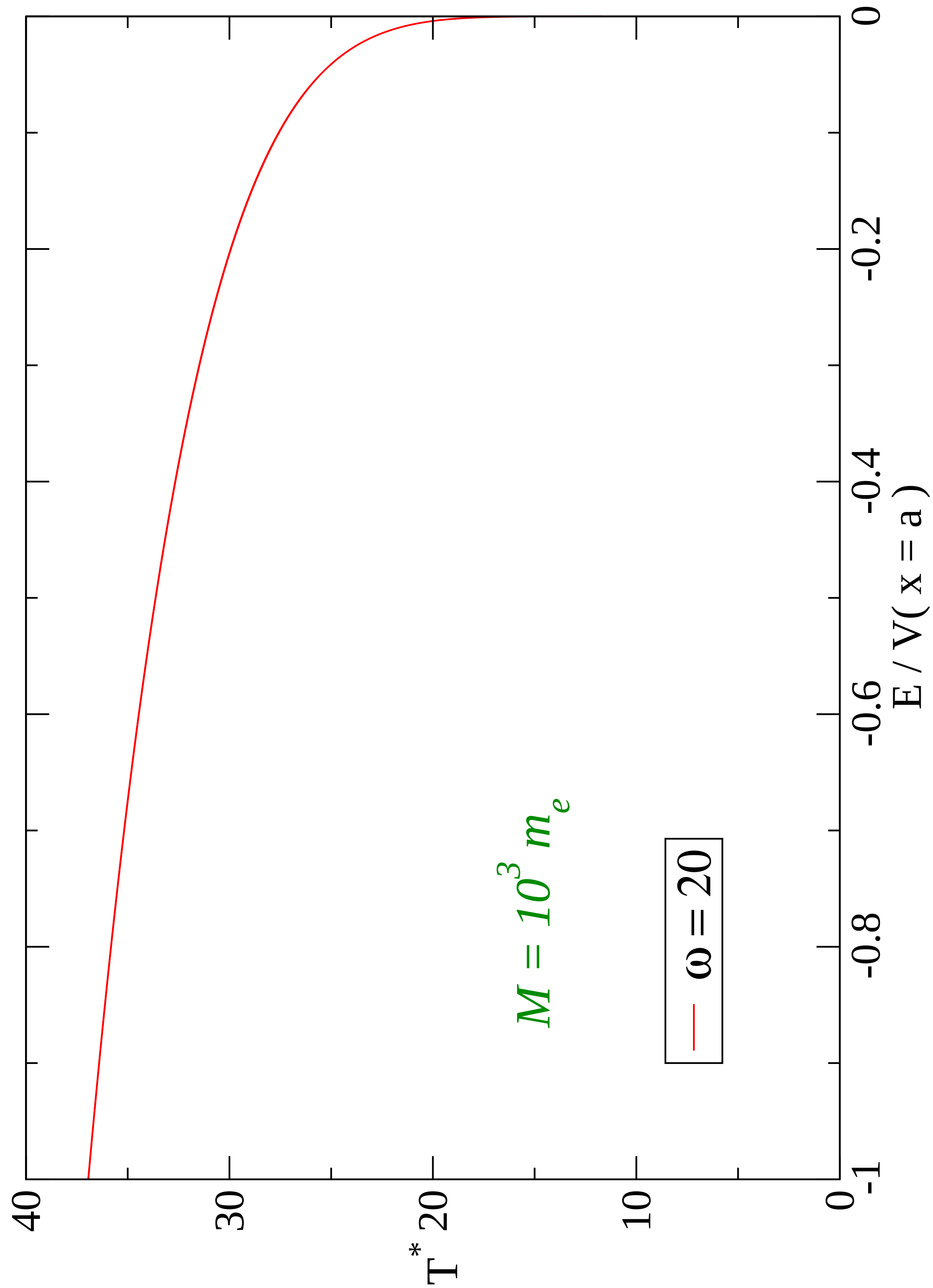

FIG. 2: (Color online)Plot of the Temperature (in Kelvin) versus *Classical Energy over Potential Barrier Height* ratio. ω is in meV.

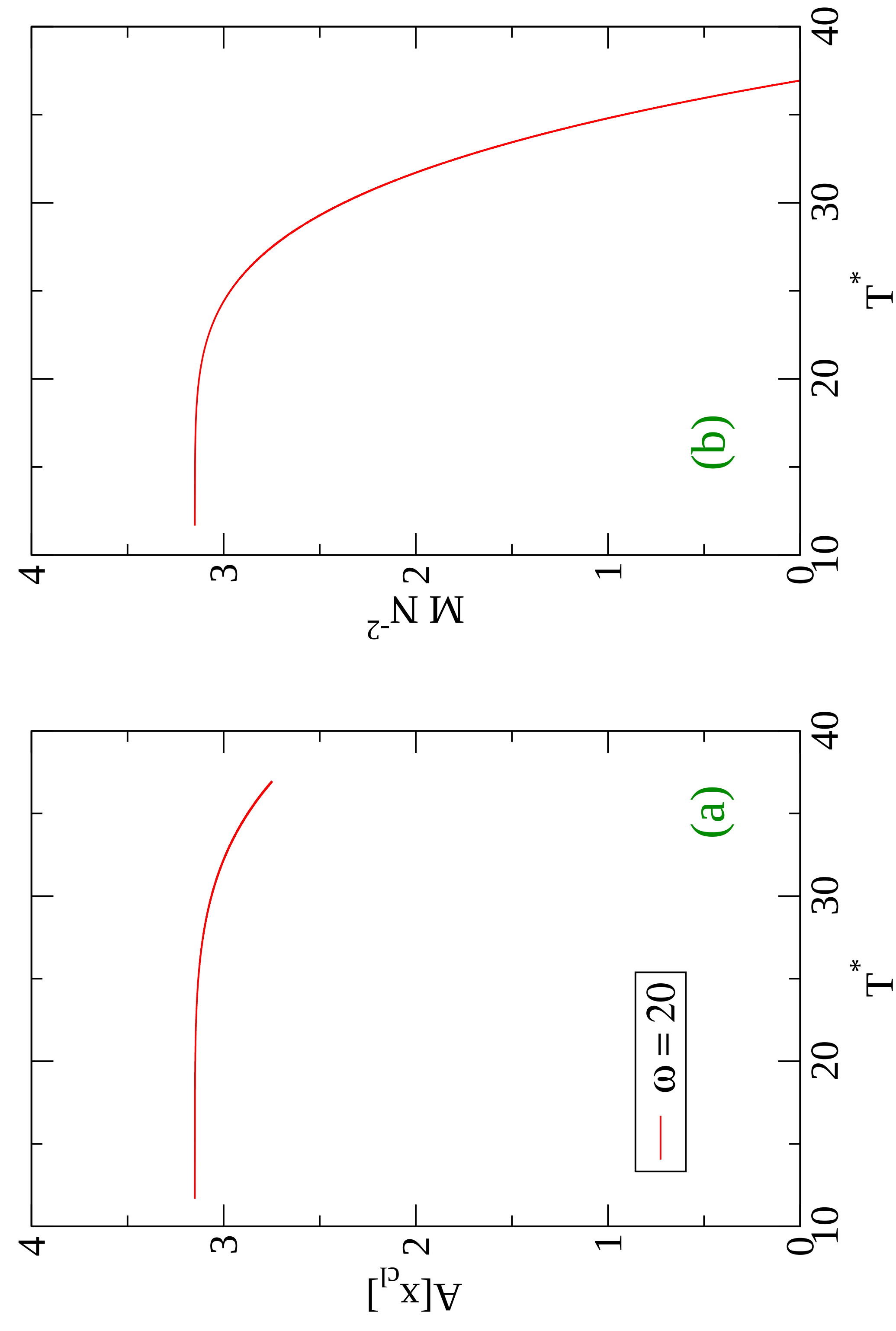

FIG. 3: (Color online) (a) Classical Action (in units $\hbar$) versus Temperature; (b) Squared Norm of the bounce velocity times particle Mass versus Temperature. ω is in meV.

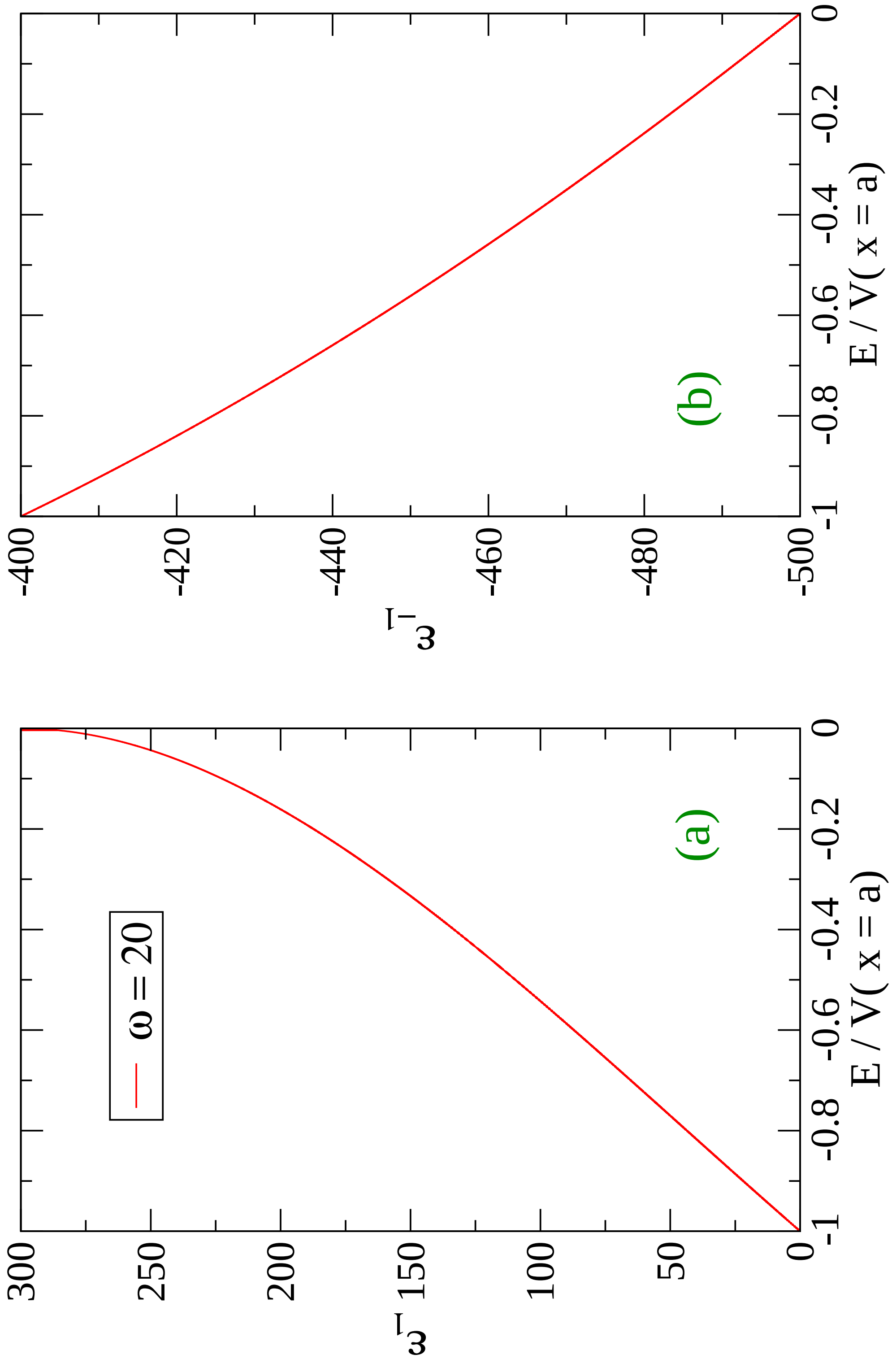

FIG. 4: (Color online) (a) Lowest lying positive and (b) Ground State quantum fluctuation eigenvalues (in units ω^2) versus *Energy over Potential Barrier Height* ratio. ω is in meV.

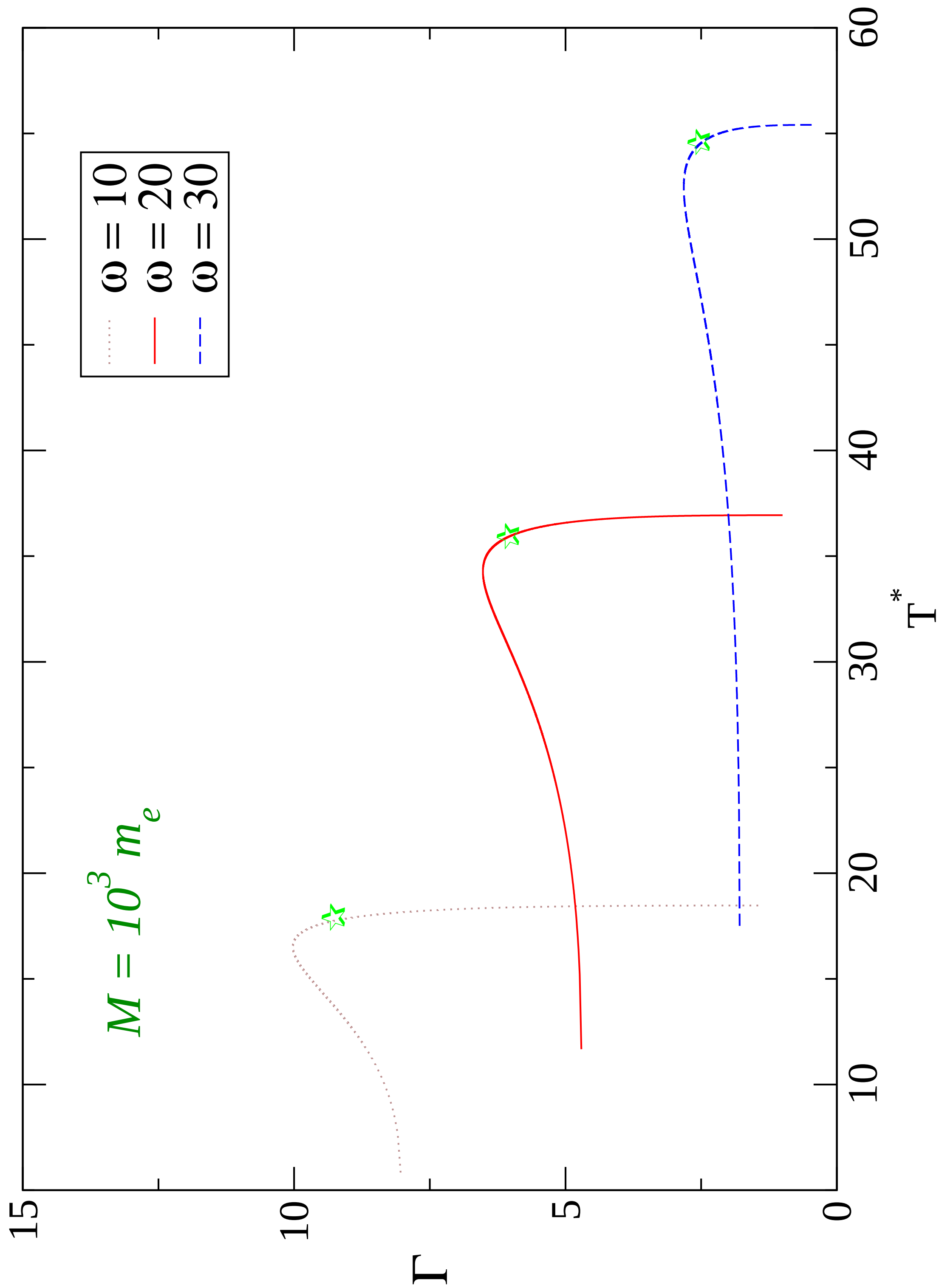

FIG. 5: (Color online) Decay rates (in meV) for a particle in metastable cubic potentials (for three oscillator energies in meV.) versus temperature up to T_c^*. The symbols mark the temperatures T_A^* in which the quantum decay rates merge with the classical Arrhenius factors.